ChemPlusChem

A Multidisciplinary Journal Centering on Chemistry

Chemistry Europe

European Chemical Societies Publishing

Reprint

WILEY-VCH

Mesostructured Electroactive Thin Films Through Layer-by-Layer Assembly of Redox Surfactants and Polyelectrolytes

Esteban Piccinini,[a] Marcelo Ceolín,[a] Fernando Battaglini,*[b] and Omar Azzaroni*[a]

Electroactive thin films are an important element in the devices devoted to energy conversion, actuators, and molecular electronics, among others. Their build-up by the layer-by-layer technique is an attractive choice since a fine control over the thickness and composition can be achieved. However, most of the assemblies described in the literature show a lack of internal order, and their thicknesses change upon oxidation-state alterations. In this work, we describe the formation of layer-by-layer assemblies of redox surfactants and polyelectrolytes that leads to the construction of mesoscale organized electroactive films. In contrast to thin films prepared with traditional redox polymers, here, the redox surfactant does not only allow the control of the film meso-organization (from 2D hexagonal to circular hexagonal phases) but it also allows the control of the number and position of the redox centers. Finally, these films show high stability and a negligible structural deformation under redox-state changes.

The precise control over the molecular organization of supramolecular self-assemblies has found a wide resonance in numerous chemistry-related fields.[1–5] The controlled integration of nano building blocks into thin films displaying meso-organized 3D functional domains constitutes a promising research area of great interest for various potential applications.[6] Many studies have demonstrated that, for certain purposes, the use of films displaying spatially organized assemblies is essential to attain specific, optimized functions.[7] This is why the development of strategies for assembling nanocomponents with a tight control over its spatial organization has become a most valuable research area within the materials chemistry community.[8] Research efforts on this scientific area are typically known as "nanoarchitectonics", a term proposed by Ariga and his collaborators.[9] Within this framework, the layer-by-layer (LbL) assembly which does not require complicated experimental setup has been of great interest as it represents a simple and versatile approach to control the vertical composition of self-assembled thin films.[10–13] In general terms, the LbL technique is based on alternate adsorption of oppositely charged materials, including linear polycations and polyanions and constitutes a well-established method for the nano construction of films integrating a large number of components of highly varied nature.[14] However, despite its intrinsic simplicity and versatility, one of the biggest limitations of LbL is its scarce control over the internal structure of the self-assembled films. Exhaustive characterization studies reported by several authors reveal that $(A/B)_n$ polyelectrolyte films present low degree of organization of the components across the film.[15] This ill-defined nature of LbL films stems from the interpenetration of neighbouring layers and is evidenced by the absence of Bragg peaks in X-ray reflectograms (XRR).

This interpenetration effect poses a serious limitation to the application of the LbL technique when specific functional groups need to be addressed in precise spatial configurations. As a result, in order to overcome this limitation, different research groups started to explore new avenues to confer true mesoscale organization to LbL. Jonas and co-workers reported that the interpenetration between neighbouring layers in multilayer assemblies can be reduced by using polyelectrolytes bearing mesogenic groups.[16] More recently, it has been demonstrated that the use of amphiphilic molecules as mesogenic agents can lead to the meso-organization of the LbL films.[17] In this regard, we should note that a direct structural comparison between traditional polyelectrolyte/polyelectrolyte multilayers and surfactant/polyelectrolyte multilayers might be misleading given the fact that both involve different molecular systems. In one case, the interacting counterparts are exclusively polyelectrolytes in which the interpenetration of successively adsorbed layers results in local structure resembling a scrambled-egg polyelectrolyte complex.[18] On the contrary, in the other case, the presence of low molecular weight surfactants may lead to the spontaneous formation of organized domains due to self-association between the amphiphilic building blocks.

The development of synthetic strategies that use surfactants as structure-directing agents has been traditionally employed to create inorganic mesoporous films[19] or surfactant-polymer salt-complexes;[20] however, there has been much less research

[a] Dr. E. Piccinini, Prof. Dr. M. Ceolín, Prof. Dr. O. Azzaroni
Instituto de Investigaciones Fisicoquímicas Teóricas y Aplicadas (INIFTA)
Departamento de Química
Facultad de Ciencias Exactas
Universidad Nacional de La Plata (UNLP), CONICET
Diagonal 113 y 64, 1900 La Plata (Argentina)
E-mail: azzaroni@inifta.unlp.edu.ar
Homepage: http://softmatter.quimica.unlp.edu.ar
[b] Prof. Dr. F. Battaglini
INQUIMAE (CONICET)
Departamento de Química Inorgánica
Analítica y Química Física
Facultad de Ciencias Exactas y Naturales
Universidad de Buenos Aires, Ciudad Universitaria
Pabellón 2, C1428EHA Buenos Aires (Argentina)
E-mail: battagli@qi.fcen.uba.ar

Supporting information for this article is available on the WWW under https://doi.org/10.1002/cplu.202000358

on surfactant-containing LbL assemblies[21,22] that than on traditional polyelectrolyte/polyelectrolyte LbL multilayers.

Several authors have demonstrated that the use of surfactant-polyelectrolyte LbL assemblies can lead to films with remarkable functional properties.[21,22] Notwithstanding these developments, only few works have studied the mesostructural properties of these materials. Interestingly, at present, the role of surfactants in LbL assemblies is almost exclusively circumscribed to mere scaffolds or structural agents to create mesoscopic domains. However, surfactants can bear specific functions with the concomitant effect of generating meso-organized functional domains with distinct physicochemical properties within the film. Exciting opportunities are revealed when we think in this manner. Self-assembly of functional surfactants provides a complementary perspective from which to consider the manipulation of the structural and functional features LbL assemblies. Of particular interest is the development of scalable and easily implemented strategies to create organized films exhibiting redox centers in specific spatial configurations. This interest stems largely from a broad range of technological applications that require the use of electroactive films, such as sensors, electrochromic and electroluminescent display devices, light harvesting, redox mediators, or molecular electronics, among others. In this context, one of the most challenging goals in supramolecular materials science is the tailored production of dimensionally stable, complex electroactive films displaying meso-organized redox-active domains based on the control of chemical topology of the interfacial architecture.

Here, we show that the layer-by-layer assembly of redox surfactants and polyelectrolytes can drive the formation of mesoscale organized electroactive films with promising functional properties. We find that the incorporation of ferrocene-appended surfactants in LbL films leads to superlattice-like supramolecular arrays whose mesostructure varies from a circular hexagonal mesostructured to a 2D hexagonal mesostructured (Scheme 1), depending on the content of redox amphiphile in the assembly.

Interestingly, we find that the self-assembled, mesostructured, electroactive interfacial architecture is sufficiently robust to tolerate electrochemical oxidation-reduction processes without detrimental effects on its dimensional stability or even structural alterations in its meso-organization. We envision that this simple and versatile strategy for producing structurally stable "soft" electroactive thin films displaying meso-organized 3D redox-active domains will lead to a new class of supramolecular materials suitable for multiple, electrochemical, electronic and optoelectronic applications.

Multilayer films were fabricated by alternating deposition of polyacrylic acid (PAA) and the cationic surfactants hexadecyltrimethylammonium bromide (CTAB) and (ferrocenylmethyl)hexadecyldimethylammonium bromide (FcCDAB, see molecular structure in Scheme S1.a in the Supporting Information). The LbL assemblies were prepared from 1 mg/ml PAA and CTAB-FcCDAB mixed surfactant solutions with the following CTAB molar fractions $\left(X^{sc}_{CTAB}\right)$: 1, 0.9, 0.7, 0.5 and 0. The resulting multilayer assemblies are referred to as

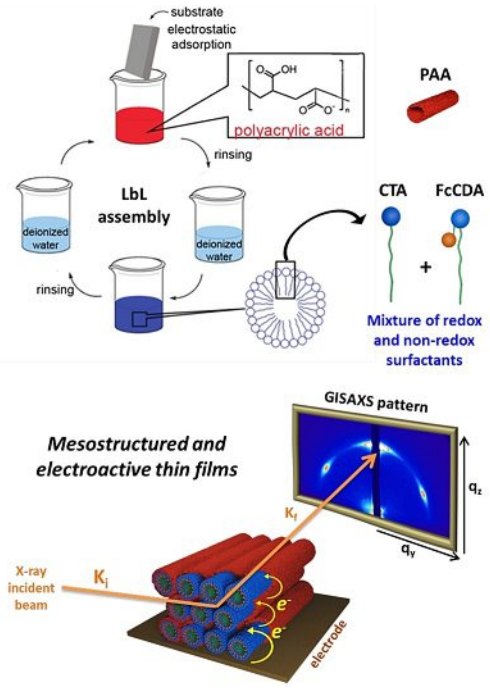

Scheme 1. Representation of the PAA/surfactants layer-by-layer assembly onto electrode surfaces, using the PAA polyanion and mixtures of redox and non-redox cationic surfactants as building blocks for the construction of mesostructured thin films with tailored electroactivity and meso-organization.

$(PAA/CTA)_n$, $(PAA/CTA_{0.9}\text{-}FcCDA_{0.1})_n$, $(PAA/CTA_{0.7}\text{-}FcCDA_{0.3})_n$, $(PAA/CTA_{0.5}\text{-}FcCDA_{0.5})_n$ and $(PAA/FcCDA)_n$, respectively. The regular deposition of $(PAA/surfactants)_n$ multilayers was corroborated by microgravimetric measurements (Table S1 in the Supporting Information). The stoichiometry of the surfactants assembled using different ratios in solution was studied by XPS. In the spectra depicted in Figure 1A it can be seen that the intensity of the signal Fe2p increases as we increase the FcCDA ratio in solution. In order to quantify the CTA:FcCDA ratio in the films, the XPS spectra of the N1s and Fe2p regions were obtained in high resolution, calibrated (using the aliphatic C1s as a reference), corrected with the baseline, integrated and applied the relative sensitivity factor determined internally from the salt spectrum of FcCDA. The ratio between CTA and FcCDA was estimated from the ratio between the relative atomic composition of N and Fe. It is important to note that the CTA:FcCDA ratio in the film is approximately equal to the ratio in the solution (Figure 1B). Therefore, these results demonstrate that the co-assembling of mixed surfactants is an attractive and simple strategy to control the concentration of functional units that are integrated into the layer-by-layer constructed film.

AFM operating in tapping mode was used to visualize the structure on the surface of the film. Contrary to traditional polyelectrolyte-polyelectrolyte LbL assemblies that exhibit a granular morphology, topographic and phase AFM images of $(PAA/FcCDA)_5$ multilayers show a smooth external surface resembling "faceted grains" in appearance (Figure 2). The formation of "grains" with smooth topography might indicate

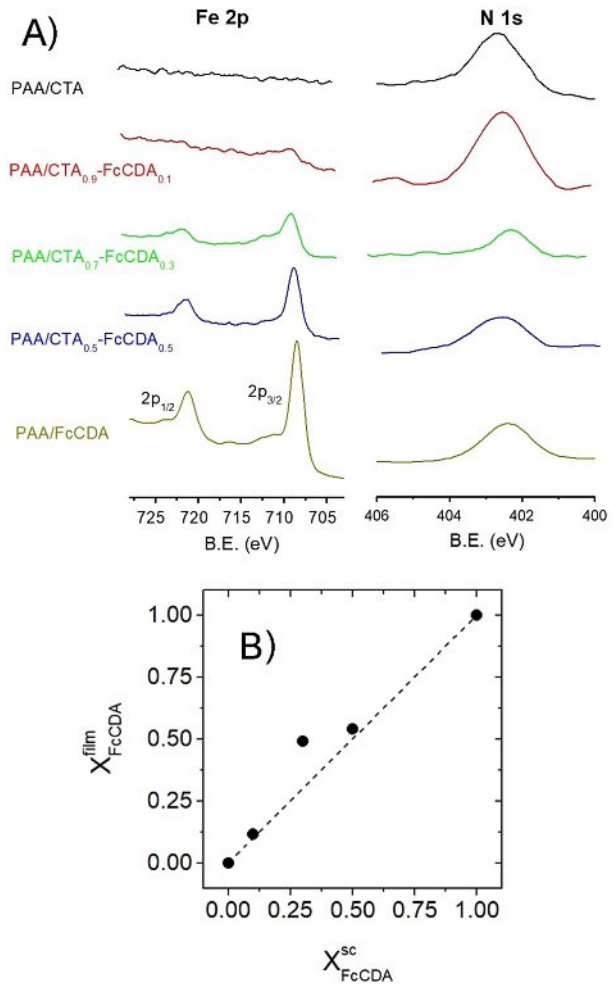

Figure 1. A) XPS spectra of the N1s and Fe2p regions for films (PAA/surfactant)$_5$ prepared from solutions of mixed surfactants in different CTA:FcCDA proportions, where a total concentration of surfactant of 2 mM is maintained. From top to bottom, molar fraction of FcCDA in solution: 0, 0.1, 0.3, 0.5 and 1. The presented XPS spectra were treated with a quadratic Savitzky-Golay filter. B) Fraction of FcCDA in the film as a function of the solution composition. Values obtained from the quantitative analysis of the XPS spectra. The trace line with slope equal to 1 is for the reader's guide.

the formation of compact, well-organized domains within the multilayer assembly.

The grazing-incidence small-angle X-ray scattering (GISAXS) technique offers a non-invasive method to study the internal nano- and mesostructure of thin films and its orientation (out-of-plane and in-plane) with respect to the substrate surface.[23] In Figure 3 it can be seen the GISAXS patterns of (PAA/surfactants)$_7$ assemblies prepared from solutions of different CTA:FcCDA ratios (additional GISAXS and QCM characterization for different compositions and different number of bilayers is included in the Supporting information file, Figure S3 and Table S1). All the assemblies showed scattering patterns with well-defined constructive interference due to diffraction phenomena, indicating the presence of periodically spaced (at the nano and mesoscale) and with spatially correlated electron density inhomogeneity. The scattering patterns of films prepared from pure CTA reveals the characteristic features of a circular hexagonal mesostructured.[24] Although this particular mesophase was previously reported for films confined in nanoporous membranes, it is important to note that, except for CTA-PAA system, the circular hexagonal mesophase has not been observed in any surfactant-polyion thin film architecture. On the other hand, films prepared entirely from FcCDA showed GISAXS patterns corresponding to a 2D hexagonal mesostructure (columns lying on the surface with hexagonal arrangement). The angular separation between the spots is 61° thus implying the presence of an almost perfect hexagonal structure. Interestingly, assemblies prepared with mixed surfactant solutions showed intermediate structure arrangements. These results indicate that the adjustable compositions of surfactants in the LbL assembly allows control over the mesostructure (e.g., circular hexagonal and 2D hexagonal). GISAXS patterns were cut along the q_z direction to obtain the out-of-plane scattering profiles (Figure 4). Table 1 describes the predominant mesophase and the characteristic periodic spacing of the (PAA/surfactants)$_7$ assemblies. From the q_z position of the Bragg peaks along q_z axis, values ranging from 3.6 to 4.3 nm were obtained for the *a* cell parameters. These results are consistent with previously reported mesostructured films prepared with quaternary ammonium surfactants of 16-alkyl tail. For instance, Antonietti et al. reported a periodic spacing of 3.52 nm for lamellar-like mesostrucured PSS-CTA "salt-complexes", while other authors reported *a* lattice values in the 4–7 nm range for hexagonal mesophased Si-CTAB mesoporous films.[25] Moreover, Picullel and coworkers reported *a* lattice values between 4–7 nm for hexagonal mesophases of "salt-complexes" prepared from PAA and CTAB.[26]

The electrochemical properties of the multilayer assemblies prepared from different CTA:FcCDA ratios were studied by cyclic voltammetry in order to assess their ability to transport electrons as well as their stability. Figure 5 shows the voltammograms of (PAA/surfactant)$_5$ assemblies prepared on gold electrodes. From the voltammograms it is appreciated that the increase in the proportion of redox surfactant produces an increase in the faradaic charge of the films. It must be noted that the (PAA/FcCDA)$_5$ assemblies dissolve during oxidation, which is observed as a decrease in the faradaic current during the voltammetric cycling (brown voltammogram in Figure 5). Similar characteristics were previously reported for assemblies of polyanions and polycations that contain a redox centers in their monomeric units.[27,28] We hypothesize that the lack of

Table 1. Values of out-of-plane q_p, z-periodic spacing, distance between column axis (*a*) as well as the predominant mesophase for the (PAA/surfactant)$_7$ assemblies prepared with different FcCDA molar fraction (X_{FcCDA}). The periodic spacing estimation error is ±0.03 nm.

X_{FcCDA}	Predominant mesophase	q_p [nm^{-1}]	z-periodic spacing [nm]	*a* cell parameter [nm]
0	Circular hexagonal	1.69	3.74	4.30
0.1	Circular hexagonal	1.85	3.41	3.92
0.3	2D hexagonal	1.93	3.27	3.76
0.5	2D hexagonal	1.99	3.17	3.64
1	2D hexagonal	2.00	3.15	3.63

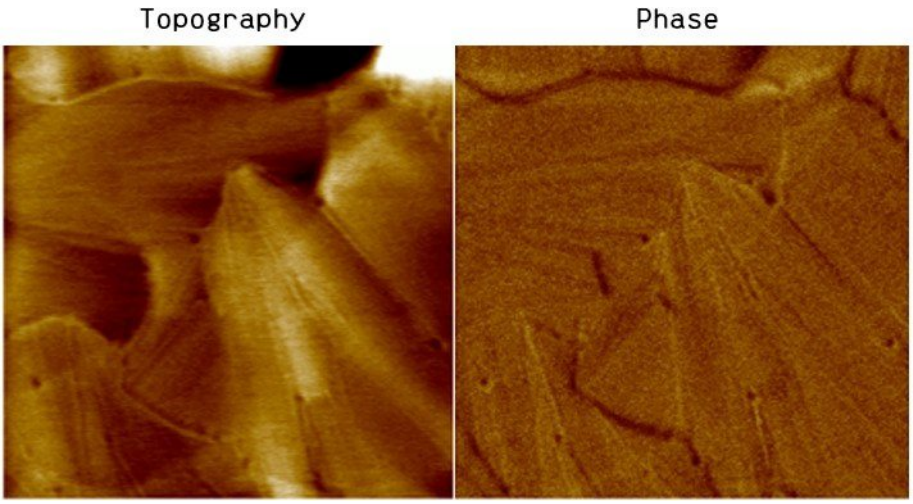

Figure 2. AFM image corresponding to topographic (left) and phase (right) imaging of $(PAA/FcCDA)_5$ multilayer assemblies (tapping mode; maximum z-scale: 60 nm; scan size: 4 μm × 4 μm).

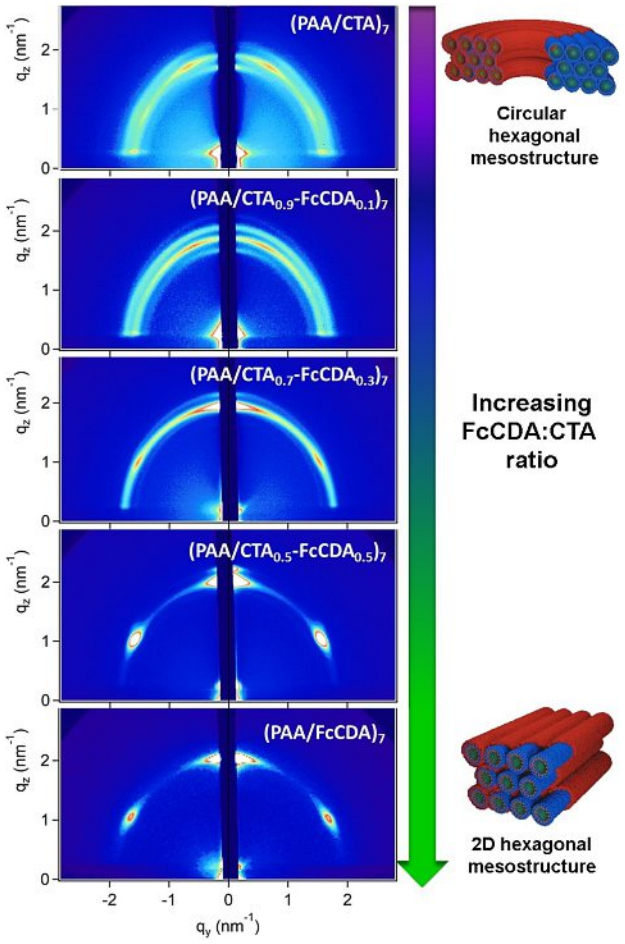

Figure 3. GISAXS patterns for $(PAA/surfactant)_7$ assemblies prepared with different CTA:FcCDA ratios. From top to bottom, molar fraction of FcCDA in solution: 0, 0.1, 0.3, 0.5 and 1. The films were prepared on Si (100) substrates modified previously with APTES. The GISAXS measurements were carried out using an incident angle (α_i) of 0.2° and a detector-sample distance of 601 mm.

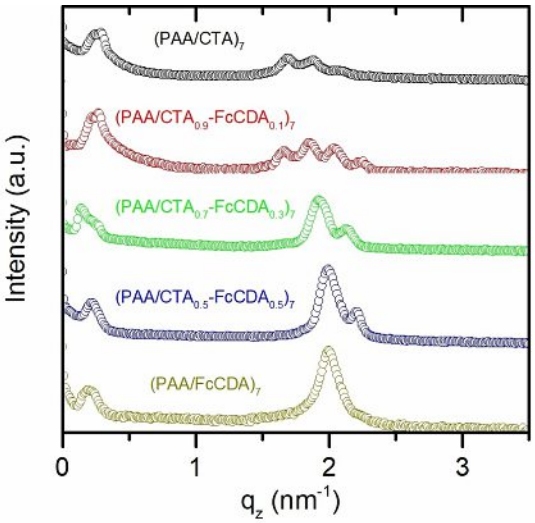

Figure 4. Out-of-plane scattering profiles extracted along the q_z direction ($q_y = 0.16\ nm^{-1}$ and with a $\Delta q_y = 0.13\ nm^{-1}$) from the GISAXS patterns for $(PAA/surfactant)_7$ assemblies prepared with different CTA:FcCDA ratios.

structural stability of our systems arises from the high concentration of redox centers. In other words, the oxidation of the redox sites results in the generation of a high density of positive charges within the assembly causing desorption due to electrostatic repulsions. Although the electrochemical desorption of the film could be an attractive feature for some applications, e.g. controlled release of molecular guests,[27,28] most of the applications require highly stable electroactive films, e.g., sensors, electrochemical diodes and other devices based on molecular electronics. In this sense, the combination of redox and non-redox-active surfactants resulted in an effective and straightforward approach to decrease the redox center concentration and, thus, improve the structural stability of the films. For instance, $(PAA/surfactant)_5$ assemblies prepared with $X_{FcCDA} < 0.5$ (red and green voltammograms in Figure 5)

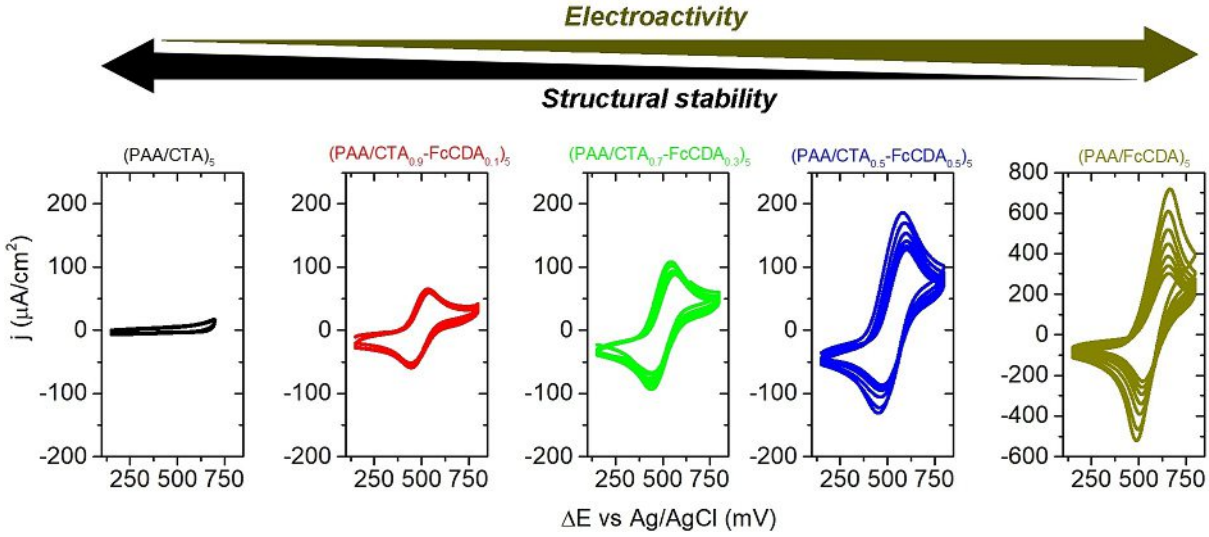

Figure 5. Cyclic voltammograms for assemblies $(PAA/surfactants)_5$ with different CTA:FcCDA ratios. From left to right: $(PAA/CTA)_5$, black; $(PAA/CTA_{0.9}\text{-}FcCDA_{0.1})_5$, red; $(PAA/CTA_{0.7}\text{-}FcCDA_{0.3})_5$, green; $(PAA/CTA_{0.5}\text{-}FcCDA_{0.5})_5$, blue; and $(PAA/\ FcCDA)_5$, brown. The voltammograms show the cycle number 1, 5, 10, 15, 20, 25 and 30. Scan rate: 50 mV/s. Electrolyte solution: 100 mM KCl.

showed highly stable electroactivity during the first 30 voltammetric cycles.

Then, we proceeded to study how the oxidation state of the $(PAA/CTA_{0.9}\text{-}FcCDA_{0.1})_n$ film affects its internal meso-organization. To achieve this goal, GISAXS studies (Figure 6) were carried out before oxidation (native state, black line), after its electrochemical oxidation (green line) and after reducing the film that had previously been oxidized (red line). To carry out these studies, the assemblies were prepared on ITO substrates previously modified with APTES. Then, a half voltammetric cycle was performed at a low scan rate (2.5 $mV\,s^{-1}$), the potential was held at 800 mV (oxidized state) and then back to 150 mV (reduced state).

Figure 6 below shows linecuts of GISAXS patterns along the q_z direction for the different oxidation conditions. A detailed

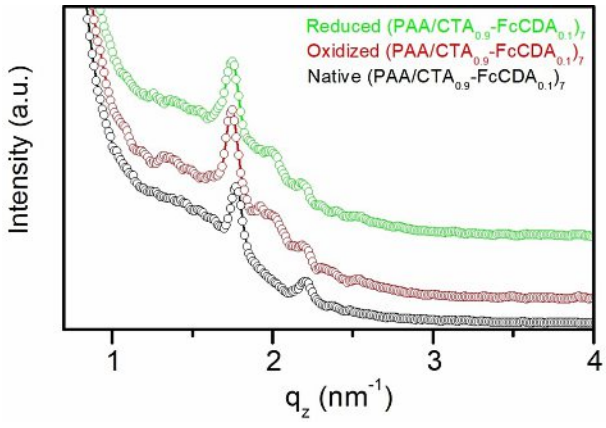

Figure 6. Out-of-plane scattering profiles extracted from GISAXS scattering patterns from cuts along the q_z direction for $(PAA/CTA_{0.9}\text{-}FcCDA_{0.1})_7$ assemblies before being oxidized (black, bottom), after oxidation of the redox centers (red, middle) and then after reduction of the centers that were previously oxidized (green, top).

characterization of the $(PAA/CTA_{0.9}\text{-}FcCDA_{0.1})_7$ system before being electrochemically oxidized (black line), after its electrochemical oxidation (green line) and after reducing the film that had been previously oxidized (red line) reveals that q_z values of maximum intensity are 1.77 nm^{-1}, 1.75 nm^{-1} and 1.75 nm^{-1}, respectively. This experimental observation indicates the film undergoes only a very mild expansion of the internal structure, i.e.: slight swelling, upon the electrochemical oxidation. Interestingly, no appreciable changes were observed after the system is reduced again. These results indicate that not only the film organization but also the mesostructural features remain almost unperturbed in the presence of the electrochemical transformation taking place into the film (i.e., reduction or oxidation) of the assemblies containing lower fraction of FcCDA. This is a non-trivial observation, especially if we consider that most of redox polymer films undergo significant structural transformations upon electrochemical cycling. We hypothesize that this particular structural stability of the mesostructured redox films stems from the cohesive forces conferred by the non-redox-active surfactants embedded into the multi-layered mesostructured. Hence, at a given redox/non-redox ratio, *i.e.*: $CTA_{0.9}\text{-}FcCDA_{0.1}$, the electrochemical generation of cationic charges into the film is not disruptive enough to cause the structural reorganization and subsequent disassembly of the multilayer. It is also interesting to note that this stability condition is attained in the case of a mesostructured assembly displaying a well-defined, reversible redox response. This implies that the remarkable structural stability of the film does not have detrimental effects neither on the charge percolation and electronic communication between redox centers nor on the electrolyte transport inside the film. This interesting experimental finding might indicate to the traditional notion that redox polymer films should display significant structural reorganization upon electrochemical cycling[29,30] due to solvent transport and charge unbalance is ***not*** an ***accurate*** portrayal of

the way some electroactive mesostructured LbL films behave. Indeed, electroactive supramolecular architectures obtained via self-assembly processes that exhibit specific components arranged in a suitable manner and reversible redox activity are one of the most coveted molecular systems for any materials chemist,[31] as they might help reduce the synthetic cost and complexity of molecular devices relying on the functions of structurally organized chemical systems.

In summary, we have demonstrated that structural control of multilayers displaying meso-organized 3D redox-active domains can be achieved via a simple polyelectrolyte/surfactant layer-by-layer technique. The strategy relies on the dual role of surfactants as functional units, *i.e.*: redox active centers, and structural units, *i.e.*: structure-directing agents. From the XPS data, it was evidenced that the co-assembling of mixed surfactants is a straightforward strategy to control the concentration of functional units that are integrated into the film. GISAXS data showed that the binary mixture of redox-active and non-redox active surfactants self-assembles into highly ordered superlattices.

Our studies show that that different meso-organized films may be obtained, ranging from a circular hexagonal mesostructure to a hexagonal 2D mesostructure, depending on the composition of the surfactant mixture. This distinctive attribute is different from previously reported polyelectrolyte-surfactant assemblies which display a stratified, lamellar configuration. In stark contrast to conventional polyelectrolyte multilayers which display a "fuzzy" organization lacking in internal structure; the assembly of surfactants leads to the formation well-defined organized mesophases within the film.

Another unique feature of these assemblies is the remarkable structural stability that they exhibit in the presence of electrochemical transformations. In particular, we found that $(PAA/CTA_{0.9}\text{-}FcCDA_{0.1})_7$ assemblies are able to display a well-defined, reversible redox response without undergoing changes in their mesostructure. This experimental observation might suggest that the traditional concept of redox active films in which electroactive assemblies display significant structural reorganization upon electrochemical cycling is no longer applicable to the case of redox-active surfactant/polyelectrolyte LbL assemblies.

As a result, this strategy constitutes a straightforward technique to create complex interfacial architectures with precise control over the spatial organization of their functional domains, even under dynamic electrochemical conditions. In this way, the fabricated self-assembled supramolecular superlattice constitutes a nanoarchitectonic design with exceptional spatial segregation of individual components into meso-organized domains. The results presented in this study may also be further extended towards the formation of other 3D supramolecular superlattice systems equipped with different functional features, e.g.: photoactivity. As such, we believe that this strategy will contribute to the rapid development of highly organized three-dimensional interfacial nanoarchitectures exhibiting tailorable mesostructural arrays and functional features, thus offering new possibilities for exploiting potentially useful collective physicochemical phenomena.

Acknowledgements

This work was supported by the following institutions: Universidad de Buenos Aires (UBACYT 20020170100341BA), Universidad Nacional de La Plata (UNLP) (PPID-X016), ANPCYT (BID PICT 2015-0801, 2016-1680, 2017-1523), and CONICET (PIP-0370). M.C., F.B. and O.A. are staff members of CONICET. E.P. acknowledges a postdoctoral fellowship from CONICET.

Conflict of Interest

The authors declare no conflict of interest.

Keywords: electroactive films · layer-by-layer assembly · mesostructured films · multilayers · surfactants

[1] a) *Supramolecular Soft Matter: Applications in Materials and Organic Electronics* (Ed.: T. Nakanishi), John Wiley & Sons, Hoboken, **2011**; b) E. Busseron, Y. Ruff, E. Moulin, N. Giuseppone, *Nanoscale* **2013**, *5*, 7098–7140; c) A. S. Picco, E. Zelaya, O. Azzaroni, M. Ceolín, *J. Colloid Interface Sci.* **2013**, *397*, 206–209; d) M. R. Hammond, R. Mezzenga, *Soft Matter* **2008**, *4*, 952–961.

[2] a) E. Moulin, J. J. Cid, N. Giuseppone, *Adv. Mater.* **2013**, *25*, 477–487; b) A. S. Picco, B. Yameen, O. Azzaroni, M. Ceolín, *Chem. Commun.* **2011**, 47, 3802–3804; c) X. Zeng, G. Ungar, Y. Liu, V. Percec, A. Dulcey, J. K. Hobbs, *Nature* **2004**, *428*, 157–160; d) C. Li, A. D. Schlüter, A. Zhang, R. Mezzenga, *Adv. Mater.* **2008**, *20*, 4530–4534.

[3] a) G. Ungar, V. Percec, M. N. Holerca, G. Johansson, J. A. Heck, *Chem. Eur. J.* **2000**, *6*, 1258–1266; b) M. L. Cortez, D. Pallarola, M. Ceolín, O. Azzaroni, F. Battaglini, *Chem. Commun.* **2012**, *48*, 10868–10870; c) A. S. Picco, W. Knoll, M. Ceolín, O. Azzaroni, *ACS Macro Lett.* **2015**, *4*, 94–100.

[4] a) S. I. Stupp, M. U. Pralle, G. N. Tew, L. Li, M. Sayar, E. R. Zubarev, *MRS Bull.* **2000**, *25*, 42–48; b) M. L. Cortez, M. Ceolín, O. Azzaroni, F. Battaglini, *Anal. Chem.* **2011**, *83*, 8011–8018.

[5] a) B. M. Rosen, C. J. Wilson, D. A. Wilson, M. Peterca, M. R. Imam, V. Percec, *Chem. Rev.* **2009**, *109*, 6275–6540; b) A. Picco, M. Kraska, H. Didzoleit, C. Appel, G. Silbestri, O. Azzaroni, B. Stühn, M. Ceolín, *J. Colloid Interface Sci.* **2014**, *436*, 243–250.

[6] a) J. Y. Park, R. C. Advincula, *Soft Matter* **2011**, *7*, 9829–9843; b) P. Liu, S. Dong, F. Liu, X. Hu, L. Liu, Y. Jin, S. Liu, X. Gong, T. P. Russell, F. Huang, Y. Cao, *Adv. Funct. Mater.* **2015**, *25*, 6458–6469; c) K. Ariga, Q. Ji, T. Mori, M. Naito, Y. Yamauchi, H. Abe, J. P. Hill, *Chem. Soc. Rev.* **2013**, *42*, 6322–6345.

[7] a) K. Ariga, Y. Yamauchi, G. Rydzek, Q. Ji, Y. Yonamine, K. C.-W. Wu, J. P. Hill, *Chem. Soc. Jpn.* **2014**, *43*, 36–68; b) K. Ariga, A. Vinu, Y. Yamauchi, Q. Ji, J. P. Hill, *Chem. Soc. Jpn.* **2012**, *85*, 1–32; c) J. Wang, J. Tang, B. Ding, V. Malgras, Z. Chang, X. Hao, Y. Wang, H. Dou, X. Zhang, Y. Yamauchi, *Nat. Commun.* **2017**, *8*, 1–9.

[8] *"Functional Supramolecular Architectures: For Organic Electronics and Nanotechnology"* (Eds.: P. Samorí, F. Caccialli), Wiley-VCH Verlag GmbH, Weinheim, **2014**.

[9] a) K. Ariga, Q. Ji, J. P. Hill, Y. Bando, M. Aono, *NPG Asia Mater.* **2012**, *4*, e17; b) O. Azzaroni, K. Ariga, *Mol. Syst. Des. Eng.* **2019**, *4*, 9–10; c) K. Ariga, M. Nishikawa, T. Mori, J. Takeya, L. K. Shrestha, J. P. Hill, *Sci. Technol. Adv. Mater.* **2019**, *20*, 51–95.

[10] a) F. X. Xiao, M. Pagliaro, Y. J. Xu, B. Liu, *Chem. Soc. Rev.* **2016**, *45*, 3088–3121; b) A. P. R. Johnston, C. Cortez, A. S. Angelatos, F. Caruso, *Curr. Opin. Colloid Interface Sci.* **2006**, *11*, 203–209; c) O. Azzaroni, K. H. A. Lau, *Soft Matter* **2011**, *7*, 8709–8724; d) E. Maza, J. S. Tuninetti, N. Politakos, W. Knoll, S. Moya, O. Azzaroni, *Phys. Chem. Chem. Phys.* **2015**, *17*, 29935–29948; e) E. Maza, C. von Bilderling, M. L. Cortez, G. Díaz, M. Bianchi, L. I. Pietrasanta, J. M. Giussi, O. Azzaroni, *Langmuir* **2018**, *34*, 3711–3719.

[11] a) M. M. De Villiers, D. P. Otto, S. J. Strydom, Y. M. Lvov, *Adv. Drug Delivery Rev.* **2011**, *63*, 701–715; b) W. A. Marmisollé, O. Azzaroni, *Nanoscale* **2016**, *8*, 9890–9918; c) G. E. Fenoy, B. Van der Schueren, J. Scotto, F. Boulmedais, M. R. Ceolín, S. Bégin-Colin, D. Bégin, W. A. Marmisollé, O. Azzaroni, *Electrochim. Acta* **2018**, *283*, 1178–1187; d) S. E.

Herrera, M. L. Agazzi, M. L. Cortez, W. A. Marmisollé, C. von Bilderling, O. Azzaroni, *Macromol. Chem. Phys.* **2019**, *220*, 1900094.
[12] a) Y. Lvov, K. Ariga, T. Kunitake, I. Ichinose, *J. Am. Chem. Soc.* **1995**, *117*, 6117–6123; b) W. A. Marmisollé, E. Maza, S. Moya, O. Azzaroni, *Electrochim. Acta* **2016**, *210*, 435–444; c) T. Berninger, C. Bliem, E. Piccinini, O. Azzaroni, W. Knoll, *Biosens. Bioelectron.* **2018**, *115*, 104; d) G. E. Fenoy, W. A. Marmisollé, O. Azzaroni, W. Knoll, *Biosens. Bioelectron.* **2020**, *148*, 111796; e) E. Piccinini, C. Bliem, C. Reiner-Rozman, F. Battaglini, O. Azzaroni, W. Knoll, *Biosens. Bioelectron.* **2017**, *92*, 661–667.
[13] a) J. J. Richardson, M. Björnmalm, F. Caruso *Science* **2015**, *348*, aaa2491 J; b) Borges, J. F. Mano, *Chem. Rev.* **2014**, *114*, 18, 8883–8942; c) A. P. Mártire, G. M. Segovia, O. Azzaroni, M. Rafti, W. Marmisollé, *Mol. Syst. Des. Eng.* **2019**, *4*, 893–900.
[14] a) I. Dewald, A. Fery, *Adv. Mater. Interfaces* **2017**, *4*, 1600317; b) M. Coustet, J. Irigoyen, T. A. García, R. A. Murray, G. Romero, M. S. Cortizo, W. Knoll, O. Azzaroni, S. E. Moya, *J. Colloid Interface Sci.* **2014**, *421*, 132–140; c) G. Decher, *Science* **1997**, *277*, 1232–1237; d) M. Lefort, G. Popa, E. Seyrek, R. Szamocki, O. Felix, J. Hemmerlé, L. Vidal, J. C. Voegel, F. Boulmedais, G. Decher, P. Schaaf, *Angew. Chem. Int. Ed.* **2010**, *49*, 10110–10113; *Angew. Chem.* **2010**, *122*, 10308–10311; e) N. E. Muzzio, M. A. Pasquale, X. Rios, O. Azzaroni, J. Llop, S. E. Moya, *Adv. Mater. Interfaces* **2019**, *6*, 1900008; f) D. Zappi, L. L. Coria-Oriundo, E. Piccinini, M. Gramajo, C. von Bilderling, L. I. Pietrasanta, O. Azzaroni, F. Battaglini, *Phys. Chem. Chem. Phys.* **2019**, *21*, 22947–22954.
[15] a) D. Korneev, Y. Lvov, G. Decher, J. Schmitt, S. Yaradaikin, *Phys. B* **1995**, *213–214*, 954–956; b) G. J. Kellogg, A. M. Mayes, W. B. Stockton, M. Ferreira, M. F. Rubner, S. K. Satija, *Langmuir* **1996**, *12*, 5109–5113; c) D. Yoo, S. S. Shiratori, M. F. Rubner, *Macromolecules* **1998**, *31*, 4309–4318.
[16] a) X. Arys, P. Fischer, A. M. Jonas, M. M. Koetse, A. Laschewsky, R. Legras, E. Wischerhoff, *J. Am. Chem. Soc.* **2003**, *125*, 1859–1865; b) X. Arys, A. Laschewsky, A. M. Jonas, *Macromolecules* **2001**, *34*, 3318–3330.
[17] a) E. Piccinini, J. S. Tuninetti, J. Irigoyen Otamendi, S. E. Moya, M. Ceolín, F. Battaglini, O. Azzaroni, *Phys. Chem. Chem. Phys.* **2018**, *20*, 9298–9308.
[18] K. Glinel, A. Laschewsky, A. M. Jonas, *J. Phys. Chem. B* **2002**,*106*,11246–11252.
[19] a) K. Ariga, A. Vinu, Y. Yamauchi, Q. Ji, J. P. Hill *Bull. Chem. Soc. Jpn.* **2012**, *85*, 1–32; b) G. J. A. A. Soler-Illia, O. Azzaroni, *Chem. Soc. Rev.* **2011**, *40*, 1107–1150; c) A. Brunsen, C. Díaz, L. I. Pietrasanta, B. Yameen, M. Ceolín, G. J. A. A. Soler-Illia, O. Azzaroni, *Langmuir* **2012**, *28*, 3583–3592; d) A. Calvo, M. C. Fuertes, B. Yameen, F. J. Williams, O. Azzaroni, G. J. A. A. Soler-Illia, *Langmuir* **2010**, *26*, 5559–5567; e) A. Calvo, B. Yameen, F. J. Williams, O. Azzaroni, G. J. A. A. Soler-Illia, *Chem. Commun.* **2009**, 2553–2555.
[20] a) C. F. J. Faul, M. Antonietti, *Adv. Mater.* **2003**, *15*, 673–683; b) C. F. J. Faul, *Acc. Chem. Res.* **2014**, *47*, 3428–3438; c) T. G. Dane, J. E. Bartenstein, B. Sironi, B. M. Mills, O. A. Bell, J. E. Macdonald, T. Arnold, C. F. J. Faul, W. H. Briscoe, *Phys. Chem. Chem. Phys.* **2016**, *18*, 24498–24505; d) T. G. Dane, P. T. Cresswell, O. Bikondoa, G. E- Newby, T. Arnold, C. F. J. Faul, W. H. Briscoe, *Soft Matter* **2012**, *8*, 2824–2832; e) Y. Okahata, G.-i. En-na, *J. Phys. Chem.* **1988**, *92*, 4546–4551; f) Y. Okahata, G.-i. En-na, K. Takenouchi, *J. Chem. Soc. Perkin Trans. 2* **1989**, *4*, 835–843.
[21] a) C. M. Dvoracek, G. Sukhonosova, M. J. Benedik, J. C. Grunlan, *Langmuir* **2009**, *25*, 10322–10328; b) M. S. Johal, B. H. Ozer, J. L. Casson, A. St. John, J. M. Robinson, H. L. Wang, *Langmuir* **2004**, *20*, 2792–2796; c) U. Manna, S. Patil, *J. Phys. Chem. B* **2008**, *112*, 13258–13262.
[22] a) M. Wu, N. An, Y. Li, J. Sun, *Langmuir* **2016**, *32*, 12361–12369; b) M. L. Cortez, A. Lorenzo, W. A. Marmisollé, C. von Bilderling, E. Maza, L. Pietrasanta, F. Battaglini, M. Ceolín, O. Azzaroni, *Soft Matter* **2018**, *14*, 1939–1952; c) M. L. Cortez, N. DeMatteis, M. Ceolín, W. Knoll, F. Battaglini, O. Azzaroni, *Phys. Chem. Chem. Phys.* **2014**, *16*, 20844–20855; d) P. K. Paul, S. A. Hussain, D. Bhattacharjee, M. Pal, *Chin. J. Chem. Phys.* **2011**, *24*, 348; e) X. Liu, L. Zhou, W. Geng, J. Sun, *Langmuir* **2008**, *24*, 12986–12989; f) M. L. Cortez, W. Marmisollé, D. Pallarola, L. I. Pietrasanta, D. H. Murgida, M. R. Ceolín, O. Azzaroni, F. Battaglini, *Chem. Eur. J.* **2014**, *20*, 13366–13374; g) M. L. Cortez, G. A. González, M. R. Ceolín, O. Azzaroni, F. Battaglini, *Electrochim. Acta* **2014**, *118*, 124–129; h) A. Lorenzo, W. A. Marmisollé, E. M. Maza, M. Ceolín, O. Azzaroni, *Phys. Chem. Chem. Phys.* **2018**, *20*, 7570–7578.
[23] a) G. Renaud, R. Lazzari, F. Leroy, *Surf. Sci. Rep.* **2009**, *64*, 255–380; b) A. Hexemer, P. Muller-Buschbaum, *IUCrJ* **2015**, *2*, 106–125.
[24] a) B. Platschek, N. Petkov, T. Bein, *Angew. Chem. Int. Ed.* **2006**, *45*, 1134–1138; *Angew. Chem.* **2006**, *118*, 1152–1156; b) J. Schuster, R. Köhn, M. Döblinger, A. Keilbach, H. Amenitsch, T. Bein, *J. Am. Chem. Soc.* **2012**, *134*, 11136–11145; c) A. Keller, S. Kirmayer, T. Segal-Peretz, G. L. Frey, *Langmuir* **2012**, *28*, 1506–1514; d) F. Marlow, I. Leike, C. Weidenthaler, C. W. Lehmann, U. Wilczok, *Adv. Mater.* **2001**, *13*, 307–310.
[25] a) D. A. Doshi, A. Gibaud, V. Goletto, M. Lu, H. Gerung, B. Ocko, S. M. Han, C. J. Brinker, *J. Am. Chem. Soc.* **2003**, *125*, 11646–11655; b) M. Antonietti, J. Conrad, A. F. Thuenemann, *Macromolecules* **1994**, *27*, 6007–6011.
[26] a) P. Ilekti, L. Piculell, L. F. Tournilhac, B. Cabane, *J. Phys. Chem. B* **1998**, *102*, 344–351; b) A. Svensson, L. Piculell, B. Cabane, P. Ilekti, *J. Phys. Chem. B* **2002**, *106*, 1013–1018; c) C. Gustavsson, J. Li, K. J. Edler, L. Piculell, *Langmuir* **2014**, *30*, 12525–12531.
[27] J. Song, D. Jańczewski, Y. Ma, L. Van Ingen, C. Ee Sim, Q. Goh, J. Xu, G. J. Vancso, *Eur. Polym. J.* **2013**, *49*, 2477–2484.
[28] J. Song, D. Jańczewski, Y. Ma, M. Hempenius, J. Xu, G. J. Vancso, *J. Colloid Interface Sci.* **2013**, *405*, 256–261.
[29] F. Mao, N. Mano, A. Heller, *J. Am. Chem. Soc.* **2003**, *125*, 4951–4957.
[30] N. Casado, G. Hernández, H. Sardon, D. Mecerreyes, *Prog. Polym. Sci.* **2016**, *52*, 107–135.
[31] M. Ruben, J. M. Lehn, P. Müller, *Chem. Soc. Rev.* **2006**, *35*, 1056–1067.

Manuscript received: May 7, 2020
Revised manuscript received: May 9, 2020
Accepted manuscript online: May 16, 2020